Electronic Supplementary Material (ESI) for ChemComm.

Supporting Information

For

Topoisomers and Aromaticity of a Redox Active 50π Core-Modified Isophlorinoid

Hosahalli S. Udaya, Ashokkumar Basavarajappa, Tullimilli Y. Gopalakrishna, and Venkataramanarao G. Anand*

Department of Chemistry, Indian Institute of Science Education and Research (IISER), Pune - 411008, Maharashtra, India.

Email: vg.anand@iiserpune.ac.in

General Experimental Methods

Column chromatography was performed on silica gel (230-400) in glass columns. ^{1}H-NMR spectra were recorded either on a JEOL 400 MHz or Bruker 400 MHz or Bruker 500 MHz spectrometer. Chemical shifts were reported as the delta scale in ppm relative to $(CH_3)_2CO$ (δ = 2.05 ppm) or CD_2Cl_2 (δ = 5.51 ppm) or $CDCl_3$ (δ = 7.26 ppm) or Tetrahydrofuran-d_8 (δ = 3.58 and 1.73 ppm). Electronic spectra were recorded on a Shimadzu UV-3600 spectrophotometer and a quartz cuvette of path length 1 cm, over the range of 300-2000nm. High Resolution Mass spectra were obtained using WATERS G2 Synapt Mass Spectrometer. Single-crystal diffraction analysis data were collected at 100K with a BRUKER KAPPA APEX II CCD Duo diffractometer (operated at 1500 W power: 50 kV, 30 mA) using graphite-monochromated Mo Kα radiation (λ = 0.71073 Å). In case of disordered solvent molecules, the contributions to the scattering arising from the disordered solvents in the crystal were removed by use of the utility SQUEEZE[1] in the PLATON software package. More information on crystal structures can also be obtained from the Cambridge Crystallographic Data Centre, CCDC 2106320, 2105357, 2105359 and 2105362 for 10(ACN), 10(benzene), 10(DMSO) and $[10]^{2+}$ respectively. Cyclic voltammetry (CV) and Differential pulse voltammetry (DPV) measurements were carried out on a BAS electrochemical system using a conventional three-electrode cell in dry CH_2Cl_2 containing 0.1 M tetrabutylammonium perchlorate (TBAP) as the supporting electrolyte. Measurements were carried out under an Ar atmosphere. A glassy carbon (working electrode), a platinum wire (counter electrode), and saturated Ag/Ag^+ (reference electrode) were used. The final results were calibrated with the ferrocene/ferrocenium couple.

Quantum mechanical calculations were performed with the Gaussian09 [3] program suite using a High Performance Computing Cluster facility of IISER PUNE. All calculations were carried out by Density functional theory (DFT) with Becke's three-parameter hybrid exchange functional and the Lee-Yang-Parr correlation functional (B3LYP) and 6-31G(d,p) basis set for all the atoms were employed in the calculations. The molecular structures obtained from single crystal analysis were used for geometry optimization. To verify the optimized structures frequency calculations were performed where no imaginary frequency was found. To simulate the steady-state absorption spectra, the time-dependent TD-DFT calculations were employed on the optimized structures. Molecular orbital contributions were determined using GaussSum 2.2.Program package. The global ring centres for the NICS (0) values were designated at the non-weighted mean centres of the macrocycles. The NICS (0) value was obtained with gauge independent atomic orbital (GIAO) method based on the optimized geometries. We calculated the Anisotropy of the current-induced density (ACID) to visualize delocalized π electrons. The ACID plots can directly display the magnitude and direction of the induced ring current when an external magnetic field is applied orthogonal to the macrocycle plane. Current density plots were obtained by employing the continuous set of gauge transformations (CSGT) method to calculate the current densities, and the results were plotted using POVRAY 3.7 for Windows. The molecular orbitals were visualized using Gauss View 4.1

Materials: Dichloromethane (CH_2Cl_2) was dried by refluxing and distillation over P_2O_5. Thiophene and pentafluorobenzaldehyde were freshly distilled prior to use. Other reagents and solvents were of commercial reagent grade and were used without further purification.

General synthetic procedure for 10 and their dication: An equimolar concentration of thiophene and pentafluorobenzaldehyde were taken in a flame-dried 250mL two neck round bottomed flask and dissolved in 100 ml dry dichloromethane and degassed with N_2 for ten minutes. Then, a catalytic amount of Boron trifluoride diethyl etherate ($BF_3{\cdot}OEt_2$) was added under dark using a syringe. After stirring for an hour, five equivalents of anhydrous $FeCl_3$ were added, opened to air and stirring continued for an additional one hour. Then few drops of triethyl amine were added and the resultant solution was passed through a short basic alumina column. This mixture was concentrated and further purified by silica gel column chromatography using CH_2Cl_2/Hexane as eluent. Dicationic salt of hexachloroantimonate was prepared as per earlier report . [2]

10: ^{1}H NMR (400 MHz, Acetone-d_6, 198 K) δ ppm 8.38 (d, *J* = 5.6 Hz, 1H), 7.70 (d, *J* = 4 Hz, 1H), 7.53 – 7.49 (m, 2H), 7.42 – 7.34 (m, 3H), 7.30 – 7.26 (m, 3H), 7.22 – 7.14 (m, 4H), 7.08 (d, *J* = 6 Hz, 1H), 7.00 (d, *J* = 6 Hz, 1H), 6.71 (d, *J* = 4.1 Hz, 1H), 6.62 (d, *J* = 3.9 Hz, 1H), 6.09 (d, *J* = 4 Hz, 1H), 5.92 (d, *J* = 5.6 Hz, 1H). **UV/vis/NIR** (CH_2Cl_2): λ_{max} nm (ε) $Lmol^{-1}\,cm^{-1}$ = 456 (137500), 650 (84200). **HR-MS** (ESI-TOF): m/z = 2609.4253 (found, $[M]^+$), (2609.7974) (Calcd. For $C_{110}H_{20}F_{50}S_{10}$).

Selected Crystal data of 10 (in Acetonitrile): $C_{112}H_{23}F_{50}S_{10}N$, ($M_r$ = 2611.86), monoclinic, space group *P21/n*, *a* = 22.655 (3), *b* = 31.011 (4), *c* = 33.670 (4) Å, $\alpha = 90^0$, $\beta = 109.552\ (2)^0$, $\gamma = 90^0$; *V* = 22291 (5) $Å^3$, *Z* = 8, *T* = 100 K , D_{calcd} = 1.581 gcm^{-3} , R_1 = 0.1213 (I > 2sigma (I)), R_w (all data) = 0.3842, GOF = 1.016;

Selected Crystal data of 10 (in Benzene): $C_{134}H_{44}F_{50}S_{10}$, ($M_r$ = 2924.29), triclinic, space group *P-1*, *a* = 10.7591 (5), *b* = 17.4880 (9), *c* = 17.8046 (7) Å, $\alpha = 63.540\ (1)^0$, $\beta = 83.089\ (2)^0$, $\gamma = 85.480\ (2)^0$; *V* = 2976.1 (2) $Å^3$, *Z* = 1, *T* = 100 K , D_{calcd} = 1.632 gcm^{-3} , R_1 = 0.0706 (I > 2sigma (I)), R_w (all data) = 0.0754, GOF = 1.265;

Selected Crystal data of 10 (in DMSO): $C_{119}H_{44}F_{50}O_5S_{15}$, ($M_r$ = 2969.43), monoclinic, space group *C2/c*, *a* = 32.114 (10), *b* = 17.231 (4), *c* = 21.376 (6) Å, α = 90, $\beta = 96.380\ (13)^0$, γ = 90; *V* = 11755 (6) $Å^3$, *Z* = 4, *T* = 100 K , D_{calcd} = 1.678 gcm^{-3} , R_1 = 0.0993 (I > 2sigma (I)), R_w (all data) = 0.3331, GOF = 1.043;

$[10]^{2+}$: ^{1}H NMR (400 MHz, Acetone-d_6, 213K) δ ppm 22.16 (s, 1H), 18.96 (s, 1H), 11.78 (d, *J* = 4.7 Hz, 1H), 11.30 (d, *J* = 4.7 Hz, 1H), 9.77 (d, *J* = 5.5 Hz, 1H), 9.30 (d, *J* = 5.5 Hz, 1H), 9.13 (d, *J* = 5.5 Hz, 1H), 8.83 (d, *J* = 4.4 Hz, 1H), 8.65 (d, *J* = 4.7 Hz, 1H), 8.57 (d, *J* = 4.7 Hz, 1H), 8.49 (d, *J* = 5.0 Hz, 2H), 8.40 – 8.33 (m, 1H), 7.95 (d, *J* = 4.4 Hz, 1H), 7.86 (d, *J* = 4.5 Hz, 1H), 7.54 (d, *J* = 5.5 Hz, 1H), 6.94 (d, *J* = 5.1 Hz, 1H), 6.86 (t, *J* = 4.8 Hz, 1H), 6.76 (d, *J* = 5.9 Hz, 1H), 6.71 (d, *J* = 4.8 Hz, 1H). **UV/vis/NIR** (CH_2Cl_2): λ_{max} nm (ε) $Lmol^{-1}cm^{-1}$ = 955 (144300), 1378 (13200), 1624 (5900). **HR-MS** (ESI-TOF): m/z = 1304.9005 (found, $[M]^{2+}$), 1304.8987 (Calcd. For $(C_{110}H_{20}F_{50}S_{10})^{2+}$).

Selected Crystal data of $[10]^{2+}$: $C_{118}H_{36}Cl_{20}F_{50}S_{10}Sb2$ (M_r = 3676.57), triclinic, space group *P-1*, *a* = 13.852 (4), *b* = 15.004 (5), *c* = 18.787 (6) Å, $\alpha = 81.290\ (8)^0$, $\beta = 69.677\ (8)^0$, $\gamma = 70.253\ (8)^0$, *V* = 3443.7 (19) $Å^3$, *Z* = 1, *T* = 100 K , D_{calcd} = 1.773 gcm^{-3} , R_1 = 0.0561 (I > 2sigma (I)), R_w (all data) = 0.1415, GOF = 1.061;

Reference:

1. A. L. Spek, PLATON, A Multipurpose Crystallographic Tool, Utrecht, The Netherlands, 2005; b)P. van der Sluis, A. L. Spek, *Acta Crystallogr. Sect. A,* **1990**, *46*, 194.
2. R. Rathore, A. S. Kumar, S. V. Lindeman, J. K. Kochi*, J. Org. Chem*. **1998,** *63*, 5847.
3. Gaussian 09, Revision D.01, M. J. Frisch, G. W. Trucks, H. B. Schlegel, G. E. Scuseria, M. A. Robb, J. R. Cheeseman, G. Scalmani, V. Barone, B. Mennucci, G. A. Petersson, H. Nakatsuji, M. Caricato, X. Li, H. P. Hratchian, A. F. Izmaylov, J. Bloino, G. Zheng, J. L. Sonnenberg, M. Hada, M. Ehara, K. Toyota, R. Fukuda, J. Hasegawa, M. Ishida, T. Nakajima, Y. Honda, O. Kitao, H. Nakai, T. Vreven, J. A. Montgomery, Jr., J. E. Peralta, F. Ogliaro, M. Bearpark, J. J. Heyd, E. Brothers, K. N. Kudin, V. N. Staroverov, R. Kobayashi, J. Normand, K. Raghavachari, A. Rendell, J. C. Burant, S. S. Iyengar, J. Tomasi, M. Cossi, N. Rega, J. M. Millam, M. Klene, J. E. Knox, J. B. Cross, V. Bakken, C. Adamo, J. Jaramillo, R. Gomperts, R. E. Stratmann, O. Yazyev, A. J. Austin, R. Cammi, C. Pomelli, J. W. Ochterski, R. L. Martin, K. Morokuma, V. G. Zakrzewski, G. A. Voth, P. Salvador, J. J. Dannenberg, S. Dapprich, A. D. Daniels, Ö. Farkas, J. B. Foresman, J. V. Ortiz, J. Cioslowski, and D. J. Fox, Gaussian, Inc., Wallingford CT, 2009.

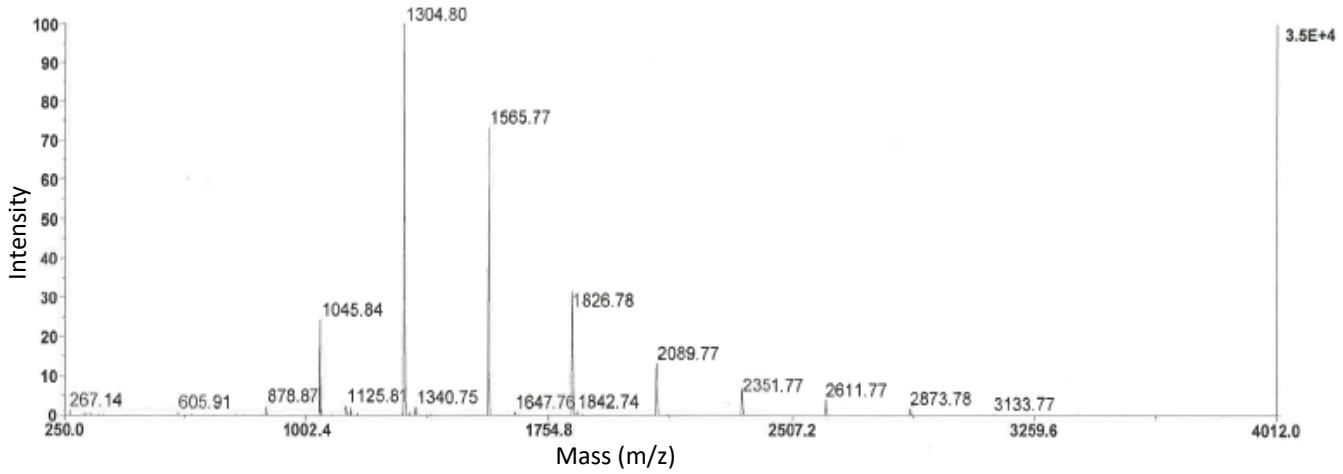

S1: MALDI-TOF/TOF mass spectrum of reaction mixture for **scheme-1**.

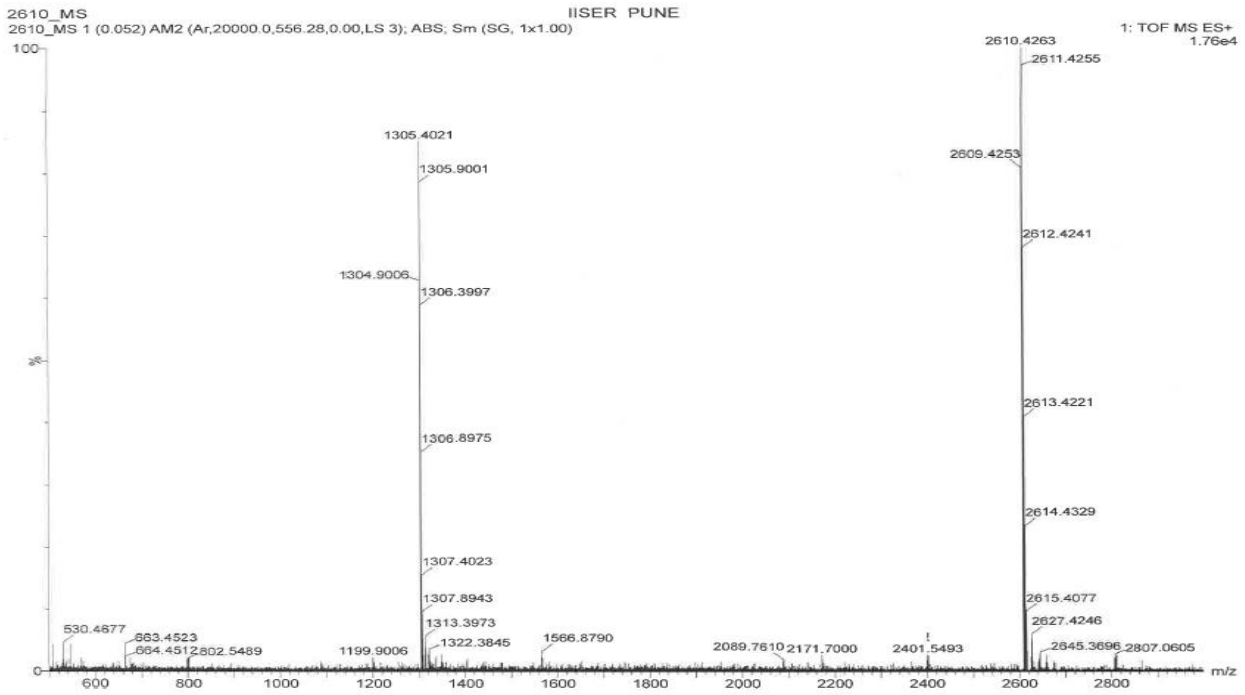

S2: HR-ESI-TOF mass spectrum of **10**.

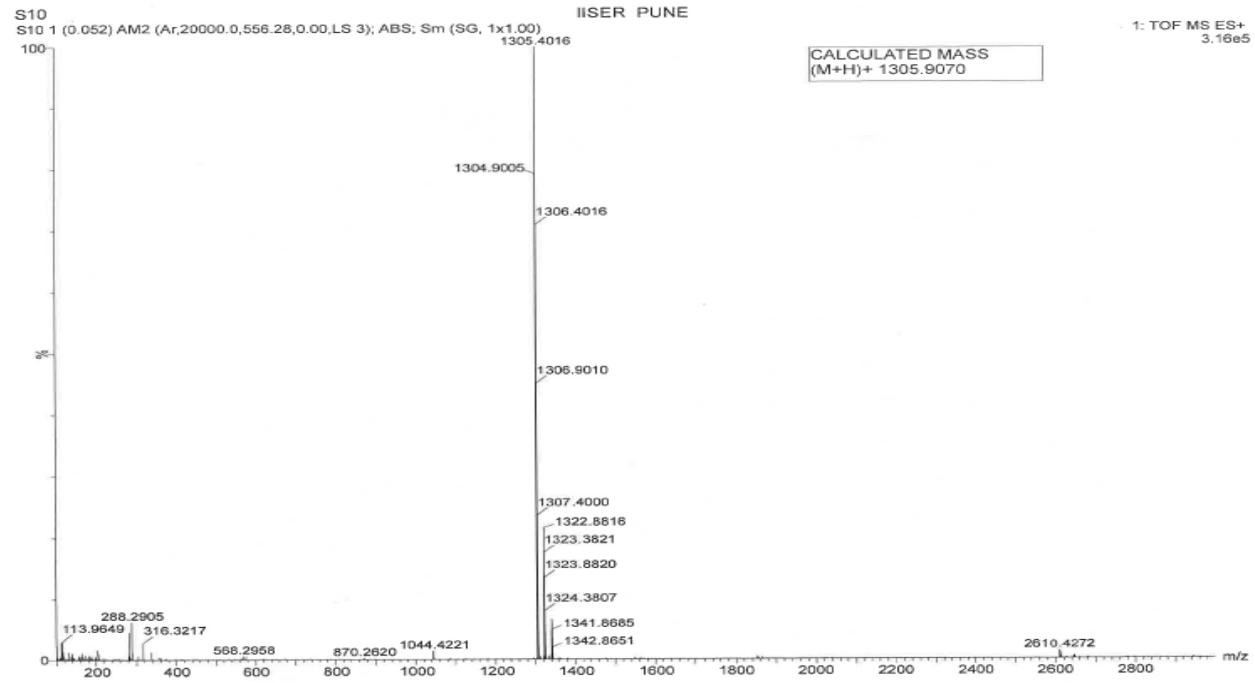

S3: HR-ESI-TOF mass spectrum of **[10]**$^{2+}$.

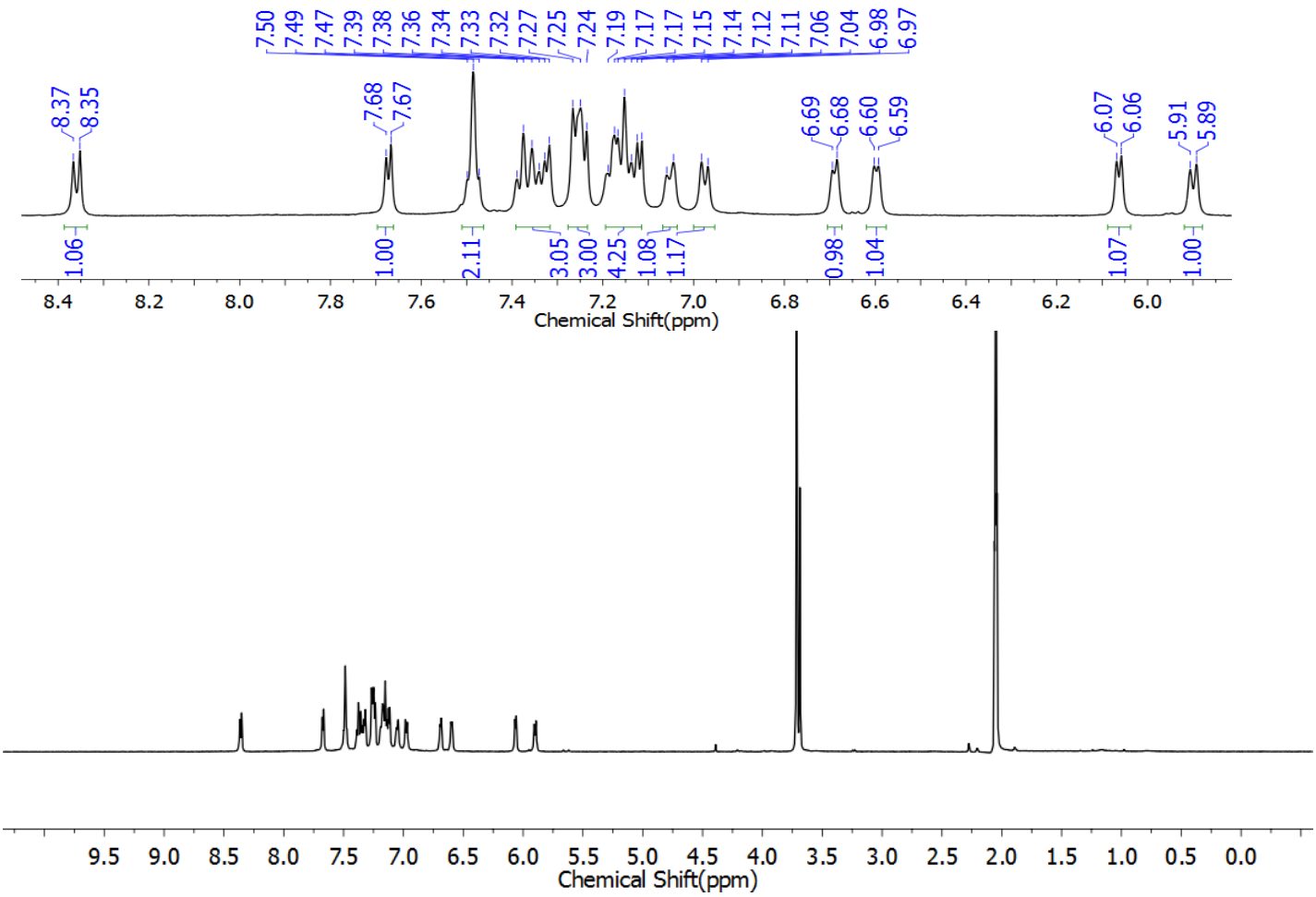

S4: ^{1}H NMR spectrum of **10** in Acetone-d_6 at 198 K.

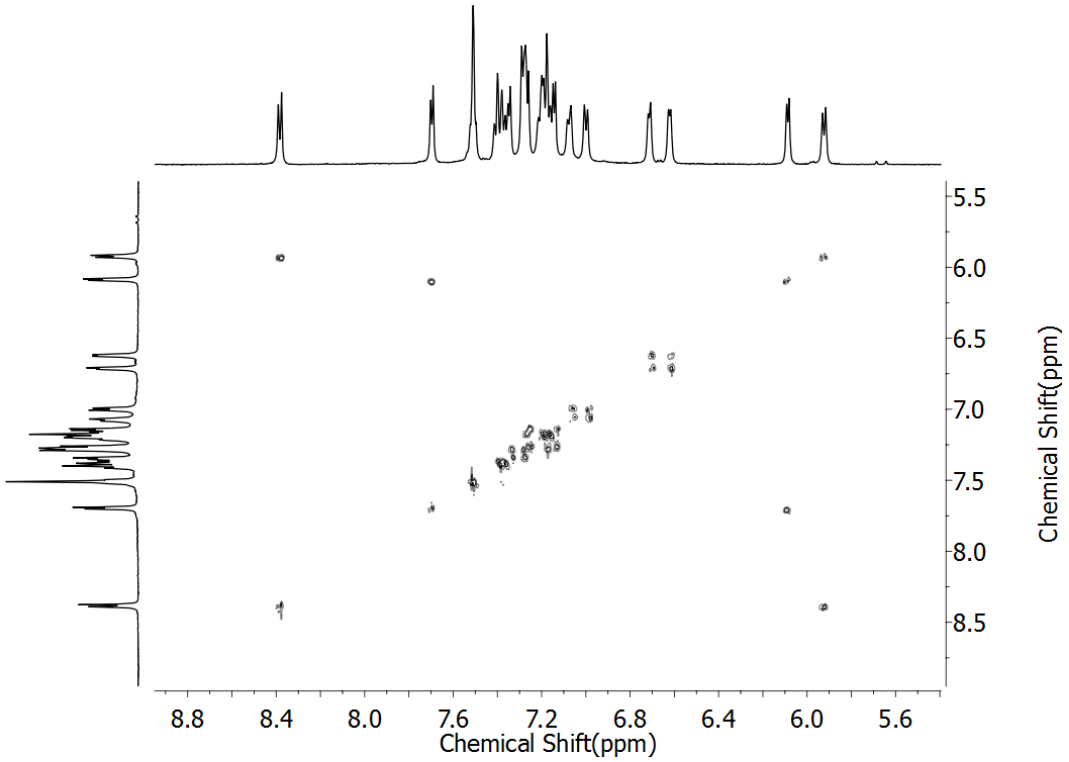

S5: ^{1}H-^{1}H COSY spectrum of **10** in Acetone-d_6 at 198 K.

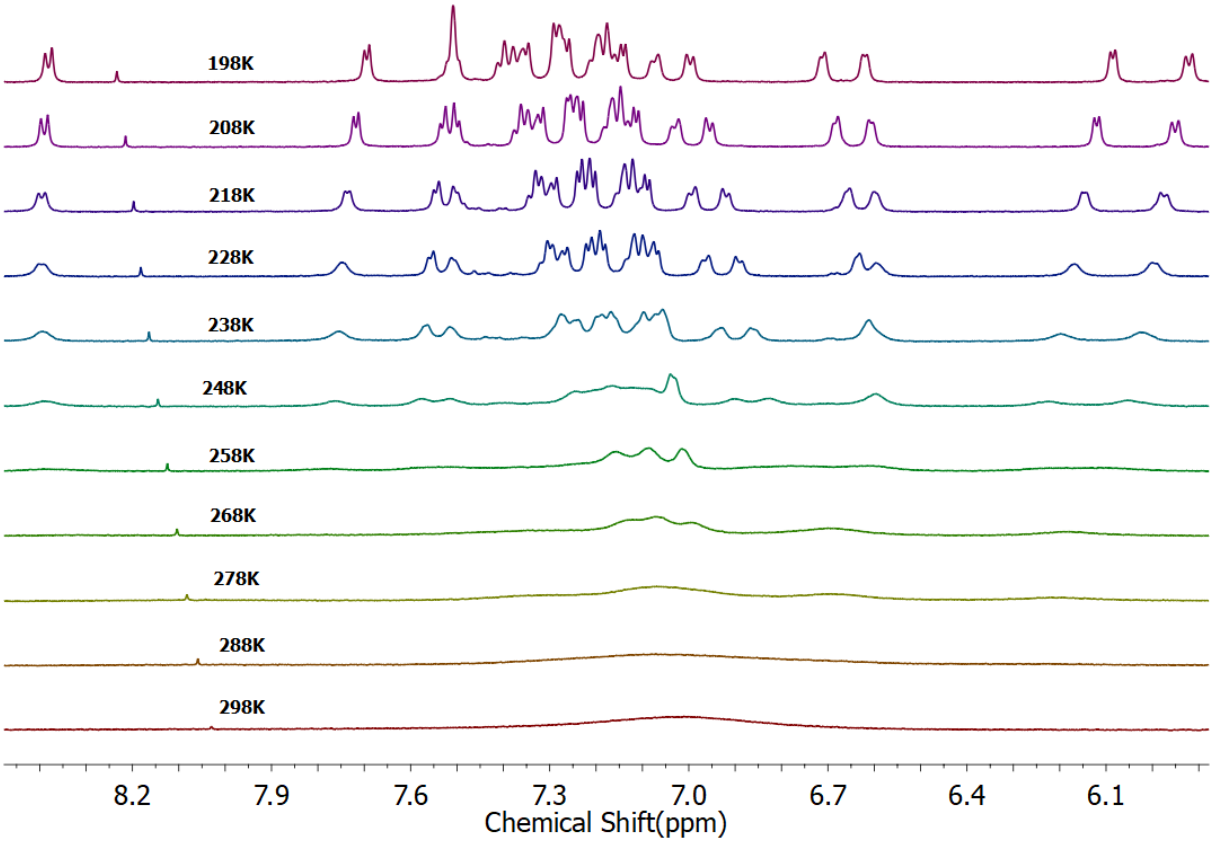

S6: Variable temperature ^{1}H NMR spectrum of **10** in Acetone-d_6.

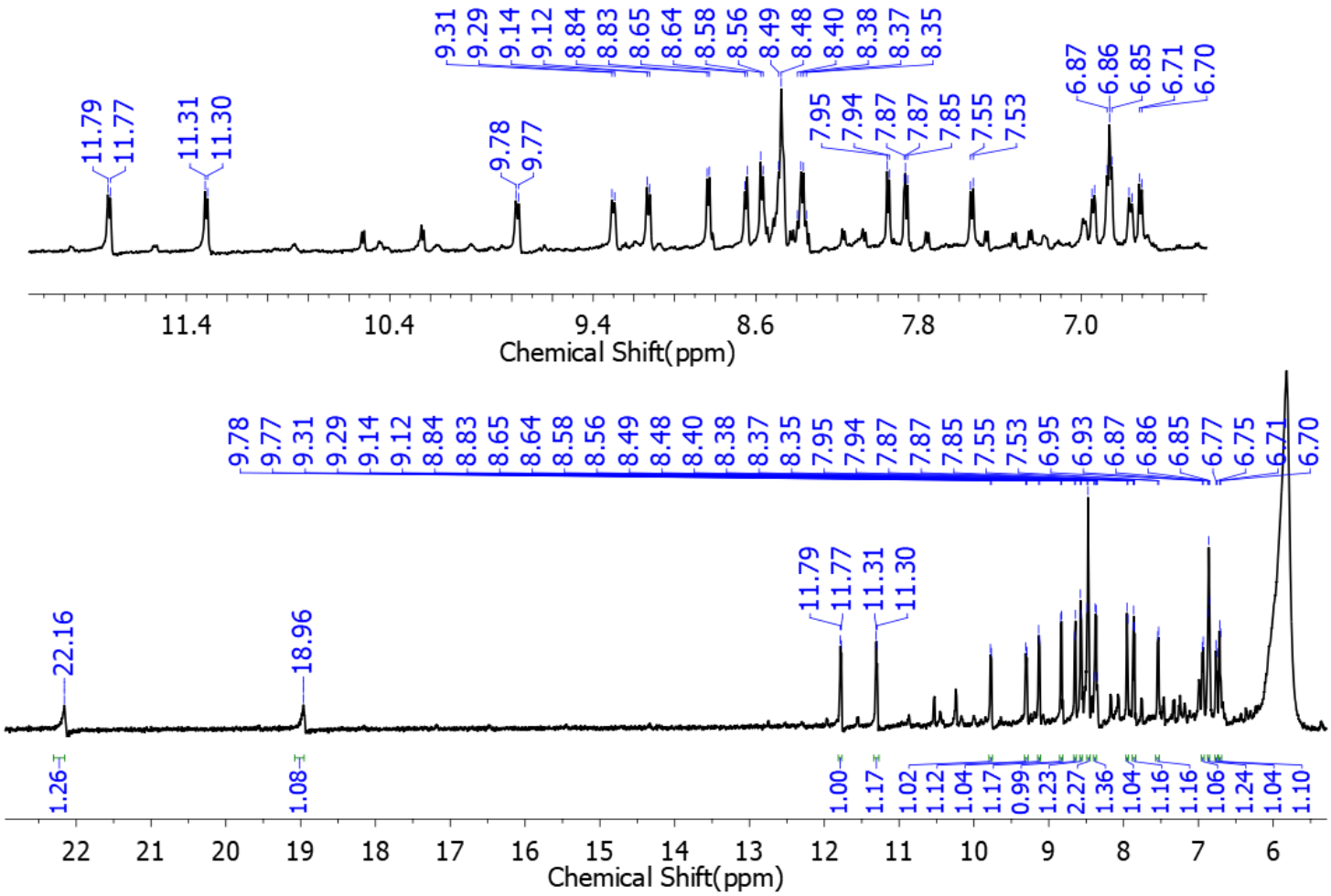

S7: ^{1}H NMR spectrum of **[10]$^{2+}$** in Acetone-d_6 at 213 K.

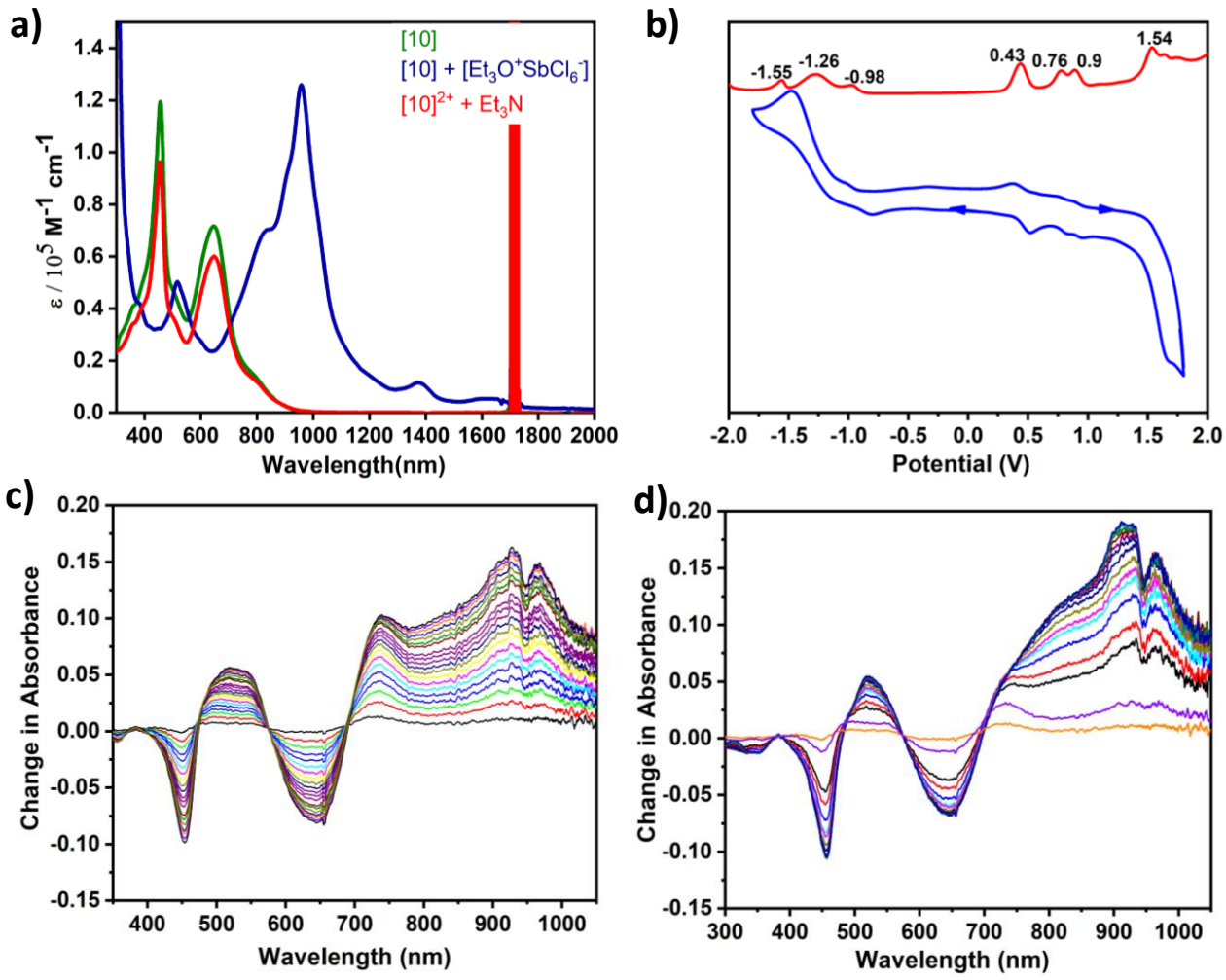

S8: (a) UV/vis/NIR absorption spectrum of 10^{-5} M solution of **10** and its oxidised species **[10]$^{2+}$** recorded in CH_2Cl_2. (b) Cyclic voltammogram (CV, blue) and differential pulse voltammogram (DPV, red) of **10** in CH_2Cl_2 (with 0.1 M $(Bu)_4NPF_6$ as the supporting electrolyte). (c and d) Change in absorption spectra of **10** after applying a potential of + 0.5 V and + 0.85 V, respectively.

(a)

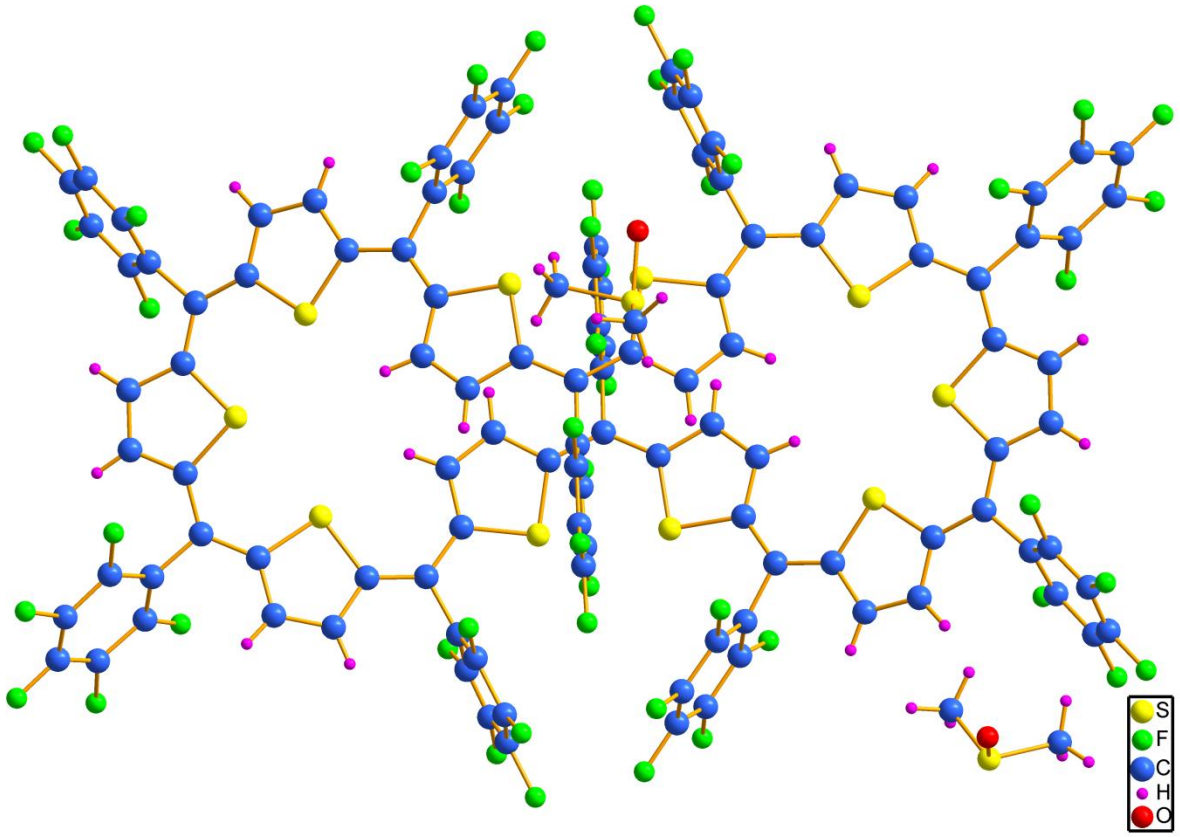

(b)

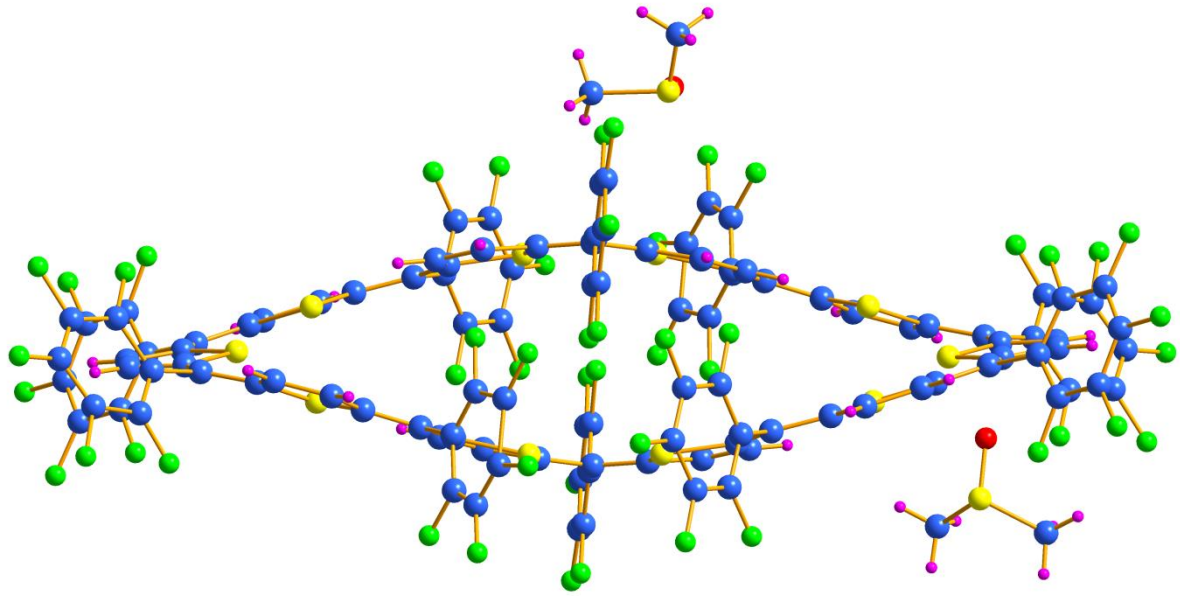

S9: Crystal structure of (a) Top view, and (b) Side view of **10** in Dimethyl sulfoxide.

(a)

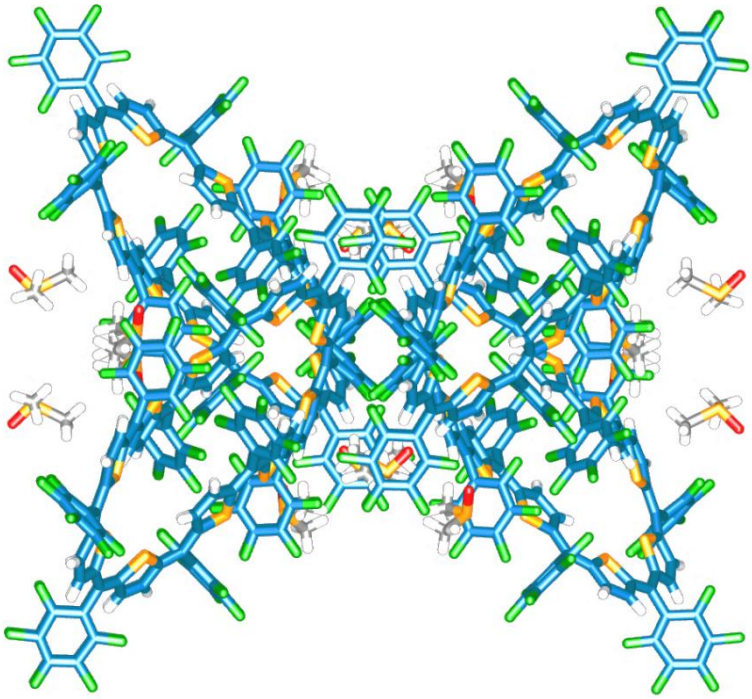

(b)

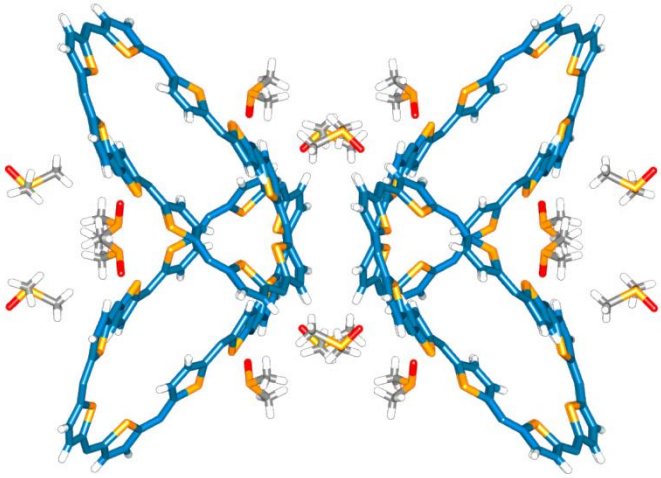

S10: Crystal packing of **10** in Dimethyl sulfoxide, showing Butterfly structure. Each oxygen of DMSO molecule interacting with β-H of thiophene, through Hydrogen bonding. (Bond length: 2.226Å and Bond angle: 159.04^0). (a) with meso pentafluorobenzene. (b) without meso pentafluorobenzene.

Macrocycle	NICS (0) ppm[a]	ACID[b]	Huckel Aromaticity
10 in Acetonitrile	-1.66 (on 4 membered ring) -0.62 (on 6 membered ring)	-	Non-aromatic
10 in Benzene	-6.75 (on both rings)	Clockwise	Aromatic
$[10]^{2+}$	+36.21 (on both rings)	Anti Clockwise	Antiaromatic

S11: Experimental and computational parameters to classify ring current effects on expanded Isophlorins. [a]Determined from quantum chemical calculations. [b]Direction of ring current obtained from ACID plots.

HOMA Calculation

All calculations were carried out through Density functional theory (DFT) with B3LYP/6-31G(d,p) basis set for all the atoms employed in the calculations. The geometry optimization was performed from the X-ray crystallographic structures. The harmonic oscillator model of aromaticity (HOMA) value calculated along the all-carbon of π-conjugation pathway.

Macrocycle	HOMA Value	Huckel Aromaticity
10 in Acetonitrile	0.532337 (0.746701)[a]	Non-Aromatic
10 in Benzene	0.924195 (0.781478)[a]	Aromatic
$[10]^{2+}$	0.787756 (0.778626)[a]	Antiaromatic

S12: HOMA values calculated using X-ray crystallographic structure [a](Values calculated for structures optimized from crystallographic data).

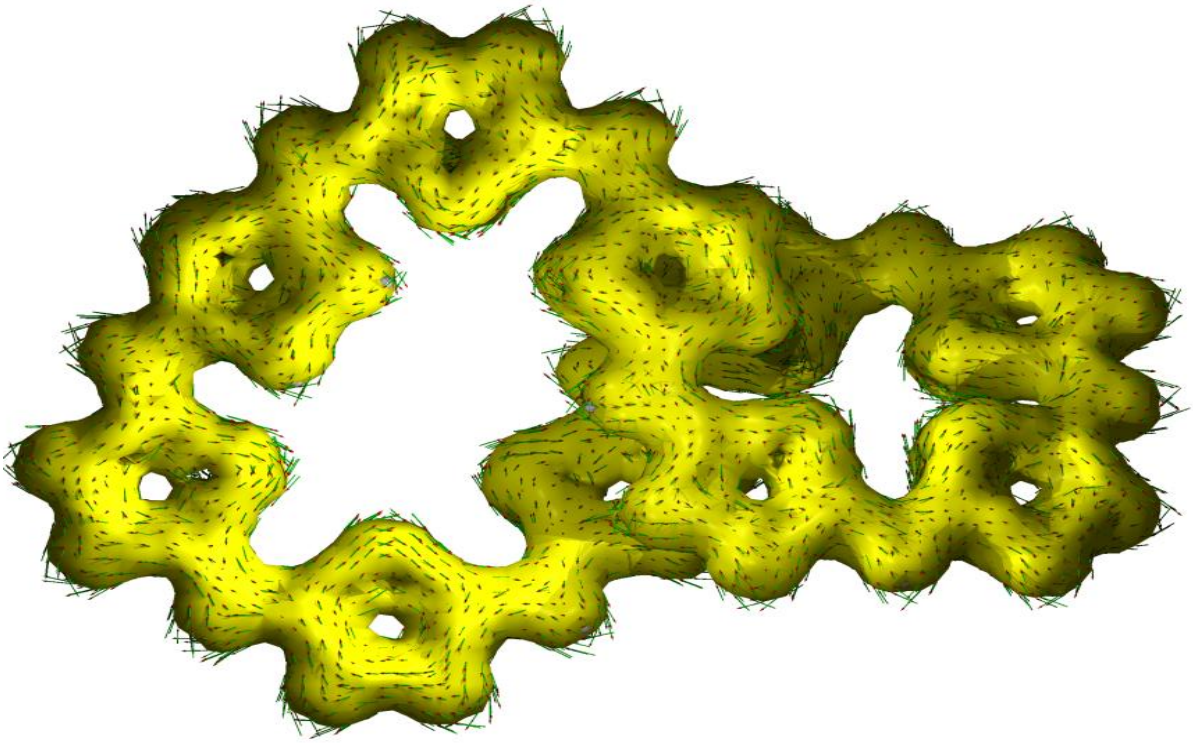

S13: ACID plot of **10** (in Acetonitrile) at an isosurface value 0.07 the external magnetic field is applied orthogonal to the macrocycle plane.

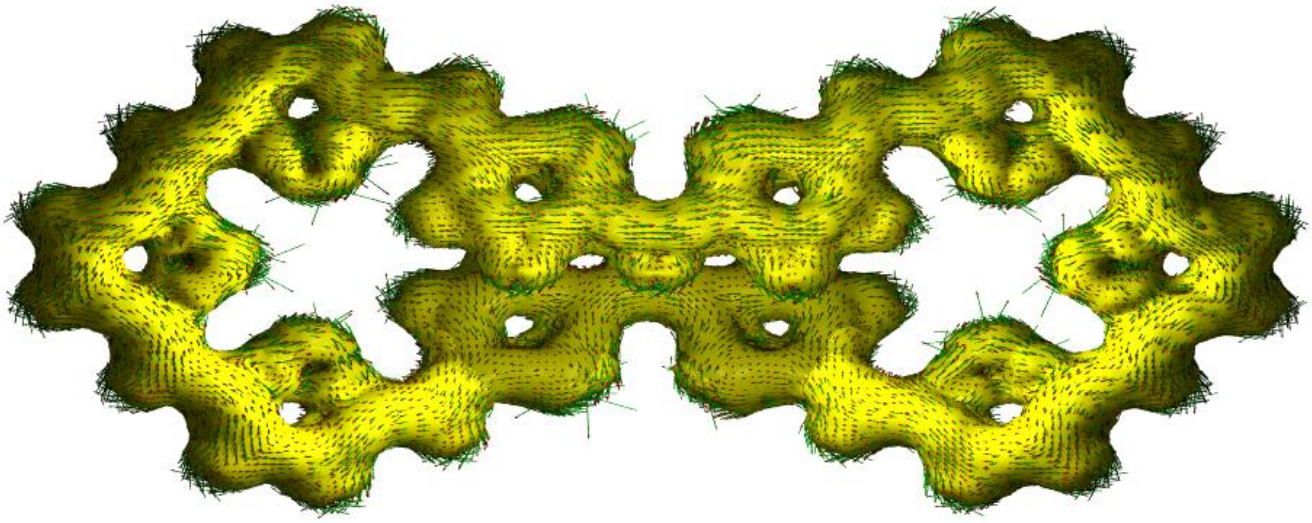

S14: ACID plot of **10** (in Benzene) at an isosurface value 0.09 the external magnetic field is applied orthogonal to the macrocycle plane.

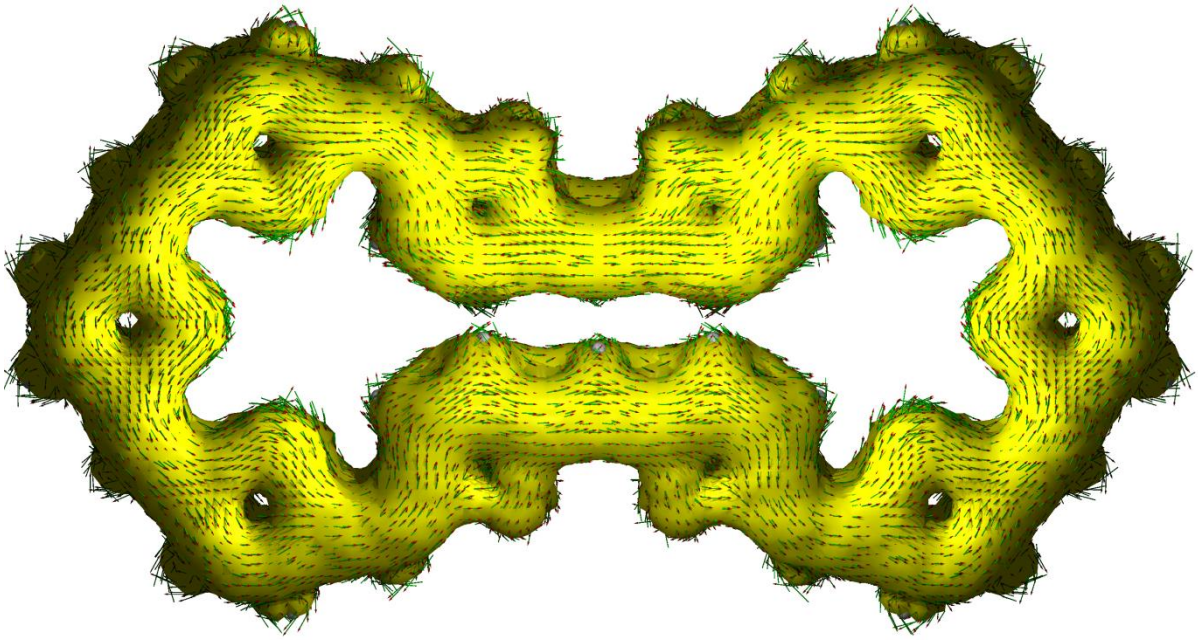

S15: ACID plot of **[10]$^{2+}$** at an isosurface value 0.06 the external magnetic field is applied orthogonal to the macrocycle plane.

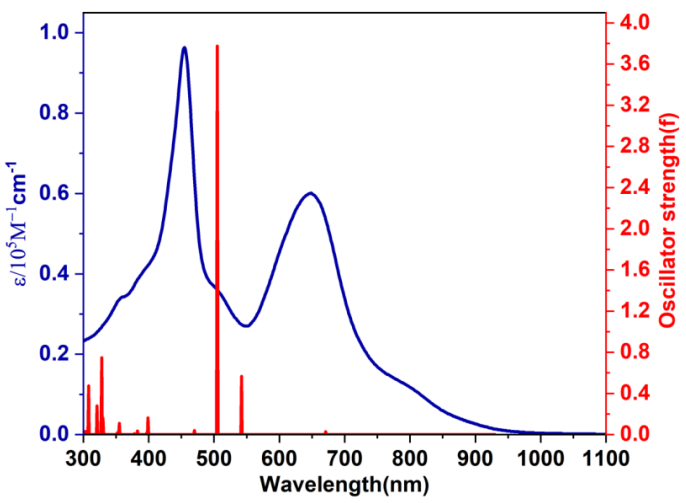

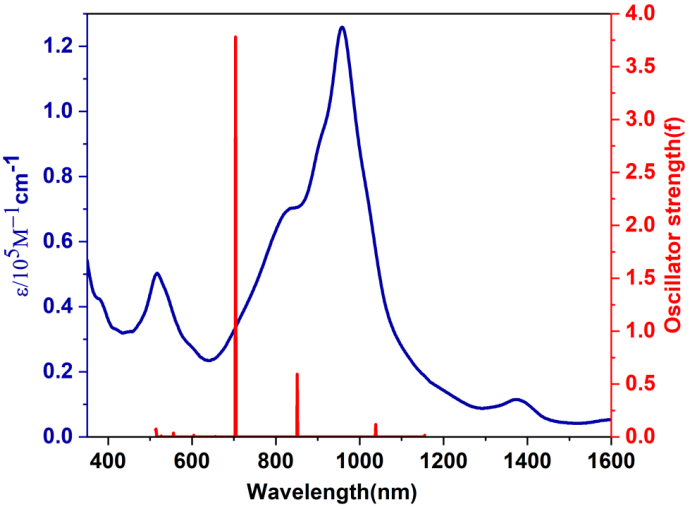

Energy (cm-1)	Wavelength (nm)	Osc. Strength(f)	Major contributions
14885.87136	671.7779402	0.0275	H-1→L+1 (32%), HOMO→LUMO (57%)
18420.21728	542.8817613	0.5665	H-1→LUMO (20%), H-1→L+1 (23%), HOMO→LUMO (11%), HOMO→L+1 (21%)
19763.13968	505.992477	3.775	H-1→LUMO (22%), H-1→L+1 (22%), HOMO→LUMO (15%), HOMO→L+1 (13%)
21250.43632	470.578573	0.0392	H-1→LUMO (40%), HOMO→L+1 (47%)
25013.03872	399.7914892	0.1634	H-2→L+1 (31%), H-1→L+2 (34%), HOMO→L+2 (11%)
25136.4424	397.8287715	0.0179	H-3→LUMO (39%), HOMO→L+3 (27%)
25205	396.7466772	0.0023	H-3→L+1 (15%), H-2→LUMO (26%), H-1→L+3 (13%), HOMO→L+2 (21%)
26080.92416	383.421996	0.0364	H-3→L+1 (15%), H-2→LUMO (14%), H-1→L+3 (22%), HOMO→L+2 (21%)
26385.80384	378.9916752	0.0102	H-3→LUMO (18%), H-2→L+1 (15%), H-1→L+2 (16%), HOMO→L+3 (25%)
28115.06848	355.6811539	0.0522	H-3→LUMO (11%), H-2→L+1 (27%), H-1→L+2 (13%), HOMO→L+3 (18%)
28163.46208	355.0699829	0.1086	H-3→LUMO (10%), H-2→LUMO (21%), H-1→L+3 (28%)
28374.7808	352.42563	0.0171	H-3→L+1 (46%), HOMO→L+2 (13%)
30249.22624	330.5869684	0.1581	H-3→L+2 (29%), HOMO→L+4 (41%)
30451.6728	328.3891846	0.7464	H-2→L+2 (39%), H-1→L+4 (28%)
31097.72736	321.5669069	0.2778	H-4→LUMO (37%), H-2→L+3 (35%)
32446.29568	308.2015925	0.4726	H-5→LUMO (12%), H-3→L+3 (50%)
32812.47392	304.762147	0.0222	H-4→L+1 (18%), H-1→L+4 (18%), HOMO→L+4 (12%)
33000.4024	303.0266079	0.0308	H-3→L+2 (18%), H-1→L+4 (12%)
33910.20208	294.8965027	0.0127	H-8→LUMO (13%), H-5→L+1 (13%)
34053.76976	293.6532452	0.0138	H-1→L+5 (22%)
34171.52752	292.6412931	0.0091	H-5→LUMO (17%), H-4→L+1 (10%)
34365.10192	290.9928806	0.0287	H-4→L+1 (10%), H-2→L+2 (14%)

34503.02368	289.829671	0.0659	H-5→L+1 (11%), H-2→L+3 (14%)
34806.29024	287.3043904	0.0059	HOMO→L+7 (21%)
34869.20192	286.7860303	0.0296	H-5→LUMO (10%)
35626.56176	280.6894493	0.0111	H-20→LUMO (13%)

S16: Selected TD-DFT (B3LYP/6-31G(d,p)) calculated energies, oscillator strengths and compositions of the major electronic transitions of **10**.

Energy (cm-1)	Wavelength (nm)	Osc. Strength(f)	Major contributions
8651.96912	1155.806252	0.0165	H-2→LUMO (27%), H-1→LUMO (13%), HOMO→L+1 (58%)
9630.3264	1038.386404	0.118	H-2→LUMO (14%), H-1→LUMO (53%), HOMO→L+2 (30%)
11749.96608	851.0662867	0.5923	H-2→LUMO (60%), HOMO→L+1 (37%)
14191.4232	704.6509613	3.781	H-1→LUMO (37%), HOMO→L+2 (63%)
15222.20688	656.9349687	0.0054	H-5→LUMO (97%)
16444.95184	608.0893454	0.0003	H-7→LUMO (95%)
16532.86688	604.8557744	0.0165	H-9→LUMO (89%)
16632.88032	601.2187792	0.0007	H-10→LUMO (89%)
17687.05424	565.3852736	0.0016	H-15→LUMO (59%), H-12→LUMO (39%)
17968.54368	556.5281293	0.037	H-15→LUMO (39%), H-12→LUMO (57%)
18949.32064	527.7234044	0.0085	H-19→LUMO (37%), H-17→LUMO (61%)
19385.6696	515.8449621	0.0007	H-20→LUMO (90%)
19387.28272	515.8020412	0.0531	H-21→LUMO (40%), H-19→LUMO (24%), H-17→LUMO (12%), H-3→L+1 (19%)
19444.54848	514.2829627	0.075	H-19→LUMO (15%), H-17→LUMO (10%), H-3→L+1 (66%)
19476.81088	513.4310777	0.0657	H-21→LUMO (56%), H-19→LUMO (20%), H-17→LUMO (13%)

S17: Selected TD-DFT (B3LYP/6-31G(d,p)) calculated energies, oscillator strengths and compositions of the major electronic transitions of **[10]$^{2+}$**.

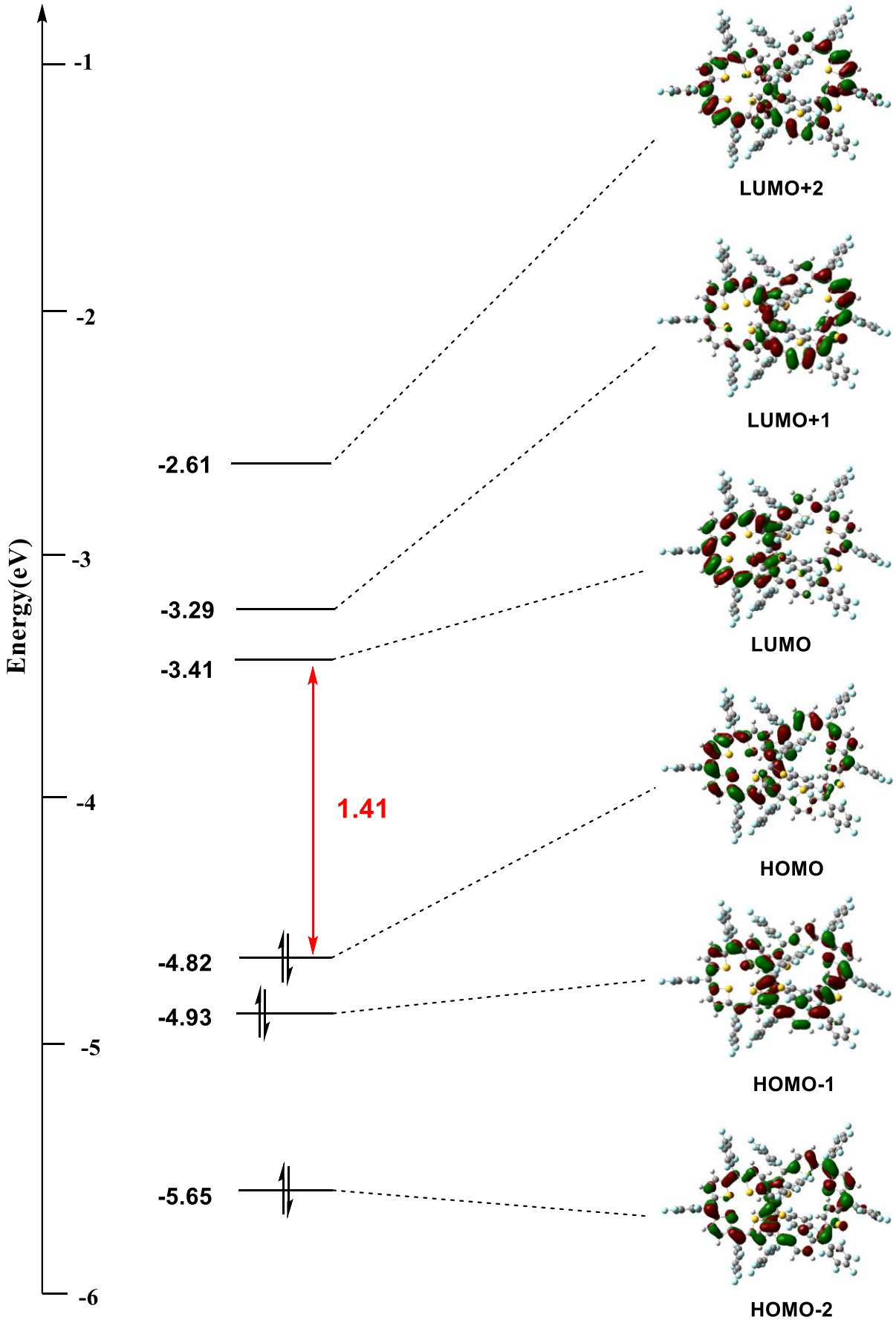

S18: Selected frontier MOs of **10** (in Acetonitrile) calculated at the B3LYP/6-31G(d,p) level.

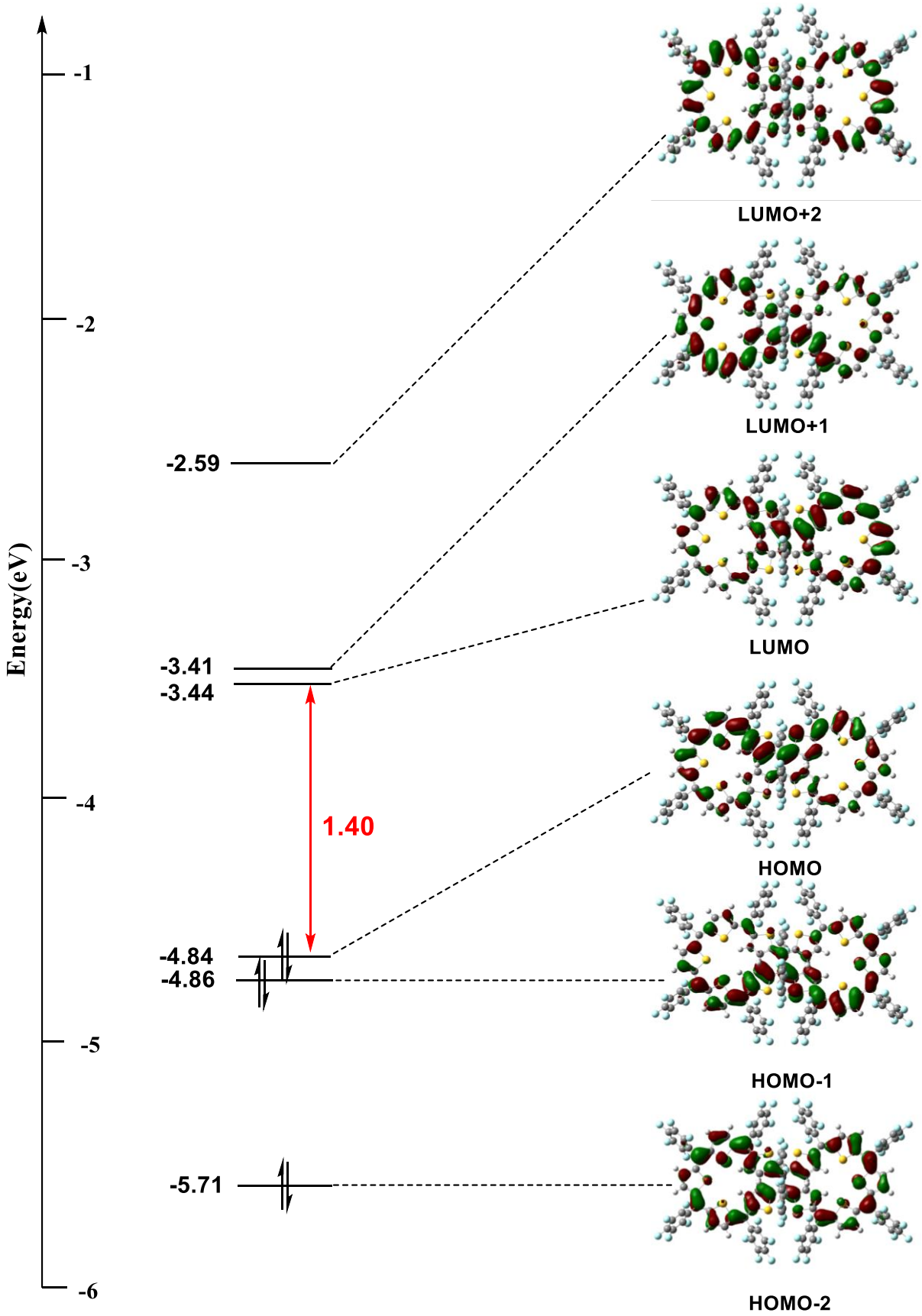

S19: Selected frontier MOs of **10** (in Benzene) calculated at the B3LYP/6-31G(d,p) level.

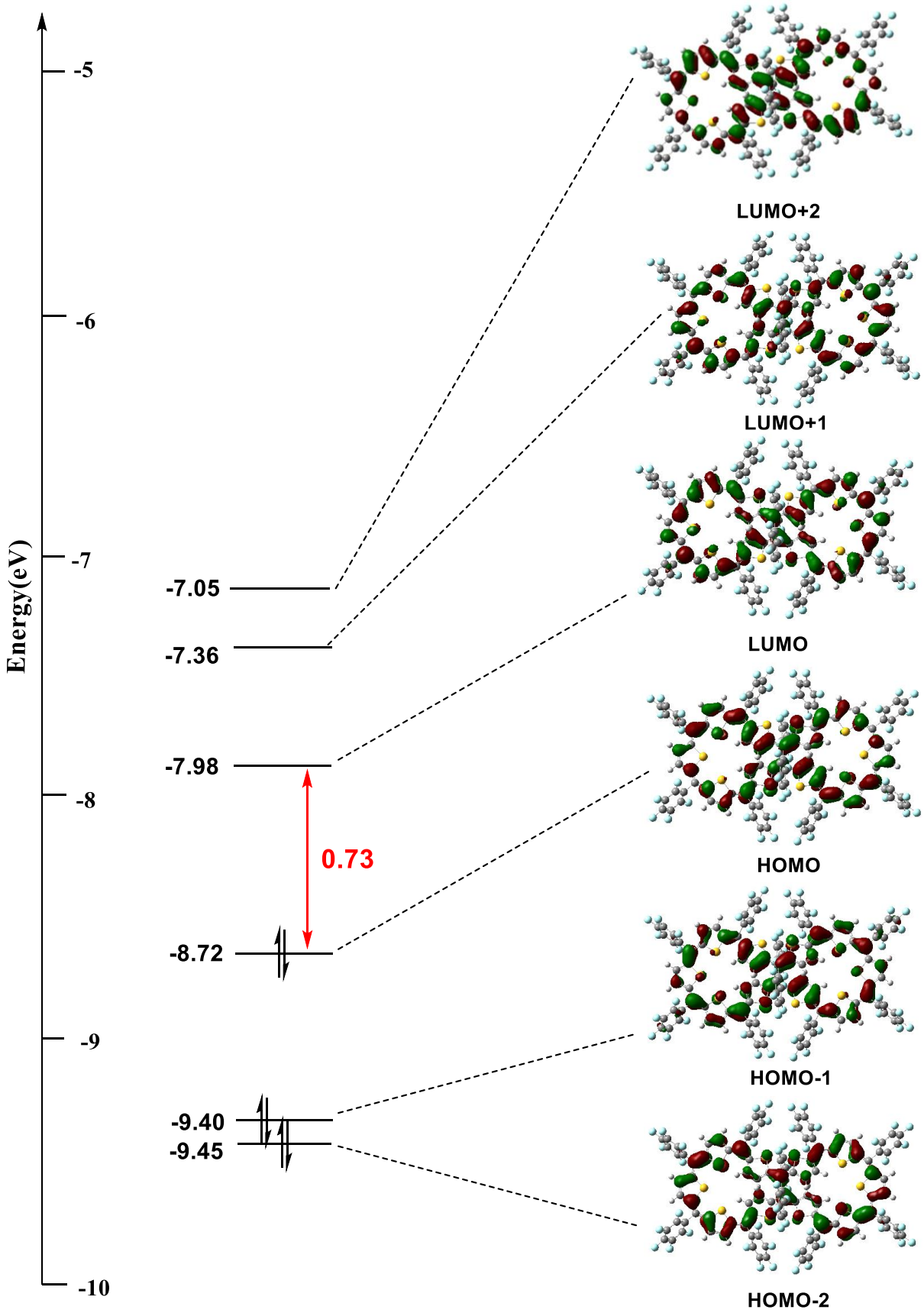

S20: Selected frontier MOs of **[10]**$^{2+}$ calculated at the B3LYP/6-31G(d,p) level.